Experimental study of temperature effect on the growth and collapse of cavitation bubbles near a rigid boundary*

LIU Xiu-mei (刘秀梅)[1], **LONG Zheng** (龙正)[1], **HE Jie** (贺杰)[1], **LI Bei-bei** (李贝贝)[1], **LIU Xin-hua** (刘新华)[1], **ZHAO Ji-yun** (赵继云)[1]**, **LU Jian** (陆建)[2], **and NI Xiao-wu** (倪晓武)[2]

1. School of Mechatronic Engineering, China University of Mining and Technology, Xuzhou 221116, China

2. Department of Applied Physics, Nanjing University of Science &Technology, Nanjing 210094, China

(Received 11 March 2013)

©Tianjin University of Technology and Springer-Verlag Berlin Heidelberg 2013

The effect of temperature on the dynamics of a laser-induced cavitation bubble is studied experimentally. The growth and collapse of the cavitation bubble are measured by two sensitive fiber-optic sensors based on optical beam deflection (OBD). Cavitation bubble tests are performed in water at different temperatures, and the temperature ranges from freezing point (0 °C) to near boiling point. The results indicate that both the maximum bubble radius and bubble lifetime are increased with the increase of temperature. During the stage of bubble rapidly collapsing in the vicinity of a solid surface, besides laser ablation effect, both the first and second liquid-jet-induced impulses are also observed. They are both increased with liquid temperature increasing, and then reach a peak, followed by a decrease. The peak appears at the temperature which is approximately the average of freezing and boiling points. The mechanism of liquid temperature influence on cavitation erosion is also discussed.

Document code: A **Article ID:** 1673-1905(2013)04-0317-4

DOI 10.1007/s11801-013-2422-y

Cavitation dynamics have an important role in physical developments in the last century. So cavitation has important impacts for a range of research fields, such as fluid mechanics, shock wave dynamics, biophysical processes and even carbon nanotube manipulation[1-3]. The understanding of bubble motion mechanism is essential for many gas-liquid and liquid-liquid interactions. The bubble behaviour in water at room temperature has been investigated over the last several years. The temperature of liquid is one of the basic factors which determine the rate and nature of the collapse of cavitation bubbles, and hence the operation of various cavitation processes, such as the erosion of solid surfaces, induces chemical reactions. With regard to temperature effect on bubble oscillation, Hammitt[4], Plesset[5], Hattori[6,7] and Ahmed[8] have studied the influence of temperature on bubble induced impact pressure and cavitation erosion. They pointed that the erosion rate increases with the liquid temperature and reaches a peak, followed by a decrease. Moreover, Barbaglia[9], German[10] and Vazquez[11] experimentally measured single bubble sonoluminescence at different water temperatures. Moshaii[12] theoretically studied the temperature dependency of single-bubble sonoluminescence in sulfuric acid. Finch[13] and Okawa et al[14] investigated the temperature effect on single bubble velocity profile and bubble rise characteristics. But the corresponding mechanism underlying the related phenomena still remains obscure.

In this paper, the effect of temperature on the dynamics of a laser-induced cavitation bubble is studied experimentally. The growth and collapse of the cavitation bubble are measured by two sensitive fiber-optic sensors based on optical beam deflection (OBD). The mechanism of liquid temperature influence on cavitation erosion is also discussed.

Fig.1 shows the cavitation bubble generating device, which was firstly reported by us in detail[15,16]. A Q-switched Nd:YAG laser with wavelength 1.064 μm and a pulse duration of 10 ns is used to produce a single bubble. The laser beam is collimated and focused to a point with radius about 50 μm to produce the liquid electrical breakdown that generates a bubble in the distilled water. The laser beam goes through an attenuator to adjust the incident laser energy without changing its spatial distribution. An extender lens with adjustable focus, which consists of a concave lens L1 with focal length of f =50 mm and a convex lens L2 with focal length of f=150 mm, is placed in the optical path to reduce the probability of generating

* This work has been supported by the National Natural Science Foundation of China (Nos.51209203 and 51005231), the Natural Science Foundation of Jiangsu Province (No.BK2012131), the China Postdoctoral Science Foundation (No.20090461156), the Special Foundation of China Postdoctoral Science (No.201003609), the Jiangsu Planned Projects for Postdoctoral Research Funds (No.1001003A), the Fundamental Research Funds for the Central Universities (No.2010QNA23), and the Priority Academic Program Development of Jiangsu Higher Education Institutions (PAPD).

** E-mail: liuxm@cumt.edu.cn

multiple plasmas and to keep a bubble in spherical shape.

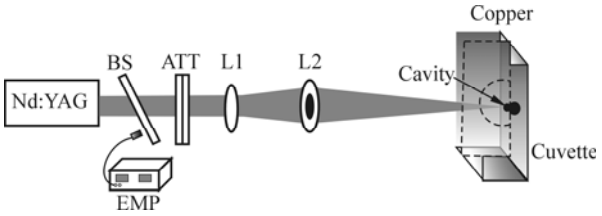

Fig.1 Basic experimental arrangement based on OBD

In the detection region, a He-Ne laser used as a probe beam is focused close to the optical breakdown region and parallel to the boundary surface, as shown in Fig.2(a). This deflected beam is then focused into a single-mode optical fiber by means of a microscope objective. Whereas, in order to detect transient behavior of liquid jets, the He-Ne laser is directly incident on the epicenter of the iron plate's rear face, where a part of the glass cuvette with a diameter of 8 mm is removed, as shown in Fig.2(b). All the reflected light is then focused by a microscope objective (f=4 mm) into a single-mode optical fiber mounted on a five-dimensional fiber-regulating stand with a spatial resolution of 0.1 μm. The light inside the fiber is transformed into an electrical pulse by a photomultiplier, fed into a two-channel digital oscilloscope, and then stored in a computer. Part of the scattered laser light is fed into a PIN photoelectric diode to generate the trigger signal. The OBD part uses an optical fiber as the sensitive receiver to detect a transient force, which increases the sensitivity of this detector.

In our experiment, the liquid temperature is controlled by electron constant temperature water bath. In order to stabilize the gas content and release the entrained gases, the test water is allowed to stand in an open atmosphere for at least 24 h. We cover the whole temperature range for distilled water from 0 °C to 90 °C. All experiments are performed at atmospheric pressure. A digital thermometer is used to record the liquid temperature. We estimate a total error of ± 1 °C, which is taken as part of the experimental error in the determination of the center temperature.

Fig.3 shows the sequence of waveforms during bubble growth and collapse detected at different distances (0 mm, 0.32 mm, 0.52 mm, 1.12 mm, 1.67 mm, 1.92 mm, 2.02 mm, 2.32 mm, 2.17 mm and 2.32 mm) in distilled water at room temperature (23 °C). It shows three major phenomena occuring during laser-matter interaction underwater: the laser-induced plasma shock wave, the cavitation bubble and the bubble-collapse-induced shock wave. Different detected distances in the experiment would result in different signals due to the variation of refractive index in the flow field. When the probe beam is very close to the target surface, such as at 0 mm in Fig.3, there is only one flat-topped wave envelope induced by an observed cavitation bubble. The refractive index gradient in the cavity region is so large that the probe beam is deflected completely out of the fiber core, which leads to the flat-topped signal. Both the laser-induced shock wave and the bubble are driven by the high-pressure plasma expansion, so the shock wave is difficult to distinguish from the expansion bubble wall in the near field, because they both expand outward at the same velocity in the initial stage. However, as the expansion increasing, the shock wave gradually detaches from the bubble wall, which is visible in Fig.3, because the shock wave velocity becomes greater than that of the particles behind it. When the detection distance is increased further, the detected signals change from "flat-top" to "semi-ellipse", and finally change to "proximal linear". Furthermore, when the probe beam is moved to a location which is outside the maximum bubble, only two shock-wave signals can be seen: one is a plasma shock wave and the other is a bubble-collapse-induced shock wave.

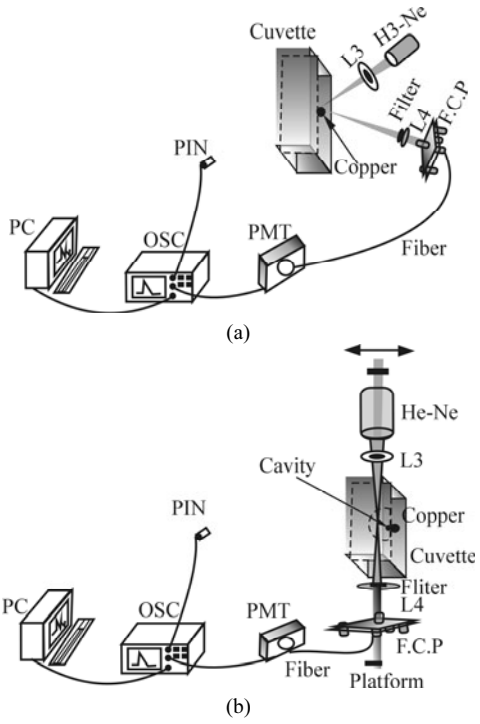

Fig.2 (a) Experimental arrangement for bubble radius evolution; (b) Experimental arrangement for cavitation erosion

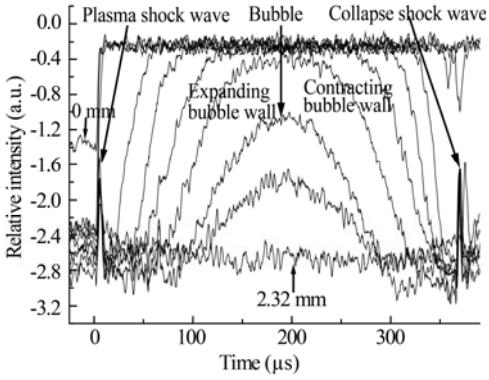

Fig.3 Typical signal detected by sensor based on OBD

By tracking arrival time of bubble walls in its expanding and contracting stages at the corresponding detection distance, temporal oscillation characteristics of a cavitation bubble near a rigid boundary can be obtained. Fig.4 shows the variation of bubble radius with time at 23 °C. Each point is the average value of five experimental data for laser pulse energy of 32.8 mJ. Some characteristic features are clearly revealed. The cavitation bubble is generated in the expansion process and expanded up to a radius of approximately R_{max}=2.22 mm. Subsequently, the bubble is decelerated sharply because of the pressure drop. And the radius is the minimum as R_{min}=0.03 mm at the instant of bubble collapse. Moreover, the expansion and collapse of the cavity are defined as the lifetime of the cavity T_{osc}=326.8 μs.

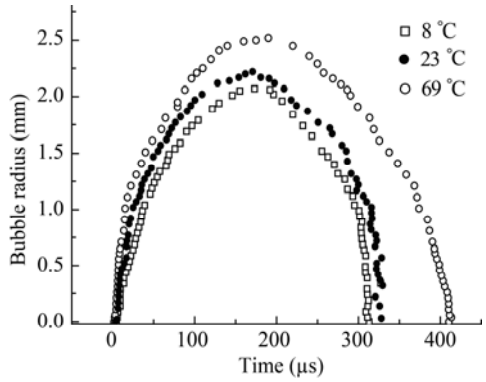

Fig.4 Time evolution of the bubble radius in distilled water at different temperatures

Furthermore, it can also be seen from Fig.4 that the liquid temperature strongly influences bubble dynamics. There are obvious changes in R_{max}, R_{min}, T_{osc} and bubble energy, when the temperature is adjusted away from 23 °C, and the detailed data are shown in Tab.1. The results show that the maximum bubble radius and bubble lifetime are increased with the increase of temperature, which are in good agreement with the results reported by Barbaglia et al[9]. At least, there are two possible reasons: Firstly, the physical properties such as viscosity and surface tension of high temperature water are quite different from those of normal-temperature water; Secondly, the vapor pressure is rapidly increased as the fluid temperature approaches the saturation temperature. The phase change at the bubble interface should become prominent in high temperature liquid. The interface condition and the bubble motion are affected by the increase of phase change rate at the interface.

Variations of the minimum radius of bubble as a function of liquid temperature are also presented in Tab.1. The minimum bubble radius is changed with the increase of temperature, but there is not a definite tendency between the minimum bubble radius and liquid temperature, which may be due to the water purity and the asphericity in the bubble collapse.

Tab.1 Bubble parameters in distilled water at different temperatures

Temperature (°C)	R_{max} (mm)	R_{min} (mm)	T (μs)	E (mJ)
0	2.02	0.063	302.0	3.45
8	2.06	0.061	306.6	3.66
15	2.11	0.050	315.4	3.93
23	2.14	0.030	321.0	4.10
28	2.17	0.041	325.0	4.28
33	2.19	0.030	327.8	4.40
39	2.20	0.040	330.0	4.46
45	2.21	0.050	336.0	4.52
51	2.23	0.045	338.8	4.64
56	2.24	0.046	339.2	4.71
63	2.26	0.040	340.6	4.83
69	2.27	0.030	341.0	4.90

According to Rayleigh's theory for spherical cavitation bubble collapse, $E_b = \frac{4}{3}\pi P_\infty R_{max}^3$, where R_{max} is the maximum radius, E_b is the bubble energy, and P_∞ is the surrounding pressure. Tab.1 shows that the bubble energy is increased with the increase of liquid temperature. In other words, the bubble collapses more violently in high temperature than in low temperature. Thus, the intended destructive effects induced by the cavitation bubbles collapse in high temperature are more serious.

As mentioned in Ref.[15], if a bubble is oscillating near a rigid wall, a jet will be formed with the direction towards the wall, so the bubble has the potential to cause boundary damage. The impact force is detected in our experiment. When a transient normal force impacts the specimen, the surface deformation is induced at the epicentre with a tiny conical protrusion. Considering that the probe light is incident on the conical protrusion with its center overlapping the conical center, the reflected beam spot is expected to change from a round shape to the shape of an annulus distribution, because part of the light shifts out of the fiber core. As a result, the transient light flux arriving at the photomultiplier is modulated. By considering the light flux variation in the fiber core, the experimental probe beam deflection signal is proved to be proportional to the transient loading force, as shown in Fig.5. The incident laser energy is 34.4 mJ, the distance L from the laser focus to the boundary is 0.122 mm, and the liquid temperature is 23 °C. There are three distinct peaks in Fig.5. Peak a denotes the laser-induced plasma ablation impact, and peaks b and c are the first and the second liquid-jet impact forces induced by cavitation bubble collapse near the solid boundary, respectively.

As liquid temperature plays a dominant role in the dynamics of cavitation bubbles, we investigate the influence of temperature on liquid-jet impact force against

the boundary. The relationship between the temperature and the actual liquid-jet impact force is shown in Fig.6. Each data point is an average of five measured values. Fig.6 shows that laser plasma ablation force and the two liquid-jet impact forces all increase with liquid temperature and reach a peak, followed by a gradual decrease. The peak appears at the approximate average of freezing and boiling temperatures. The mechanism can be reasonably explained as follows. When the water temperature is low, the gas content in water is high, which acts like a cushioning effect, and the result is that the bubble collapse velocity is decreased, thereby decreasing the liquid-jet impact force. When the temperature is above 50 °C, the cushioning effect is decreased due to reduced gas content, thus increasing the liquid-jet impact force. But the saturation vapor pressure is also increased, which reduces the liquid-jet impact force and cavitation erosion markedly[5]. Either of these two factors plays a significant role at high temperature.

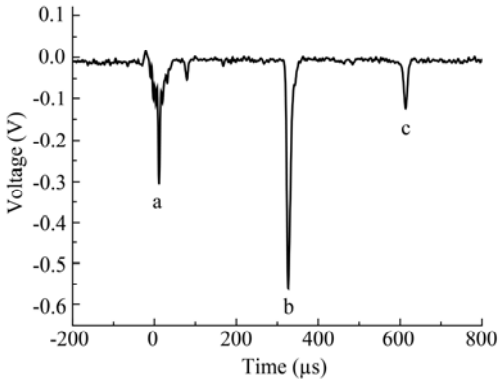

Fig.5 Typical signal detected by the OBD method at 23 °C

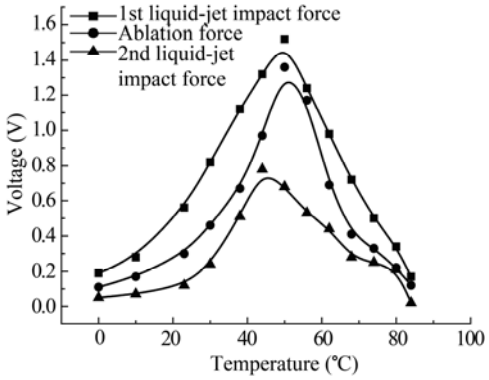

Fig.6 Signal amplitude of liquid-jet impact as a function of water temperature

In conclusion, these experiment results show that the cavitation behavior and its damage to material are obviously affected by the liquid temperature. Both the maximum bubble radius and bubble lifetime are increased with the increase of liquid temperature. In addition, when a bubble collapses near a rigid wall, underwater targets are impacted by laser-induced ablation force and the first and the second liquid-jet impact forces induced by cavitation bubble collapse. They all initially increase with temperature from 0 °C to 50 °C, reach a maximum at about 50 °C, and then decrease with the further increase of temperature to 90 °C. These results help to better understand the cavitation erosion and optimize laser parameters in the fields of laser ophthalmology and underwater laser processing.

References

[1] D. Faccio, G. Tamošauskas, E. Rubino, J. Darginavičius, D. G. Papazoglou, S. Tzortzakis, A. Couairon and A. Dubietis, Phys. Rev. E **86**, 036304 (2012).

[2] Li Sheng-yong, Liu Xiao-ran, Wang Jiang-an, Zong si-guang, Shen Zhong-hua and Ni Xiao-wu, Journal of Optoelectronics·Laser **23**, 1206 (2012). (in Chinese)

[3] Li Sheng-yong, Liu Tao, Wang Jiang-an and Zong Si-guang, Journal of Optoelectronics·Laser **23**, 2440 (2012). (in Chinese)

[4] F. G. Hammitt, Cavitation and Multiphase Flow Phenomena, McGraw-Hill, New York, 1980.

[5] M. S. Plesset, Trans. ASME J. Basic Eng. **94**, 559 (1972).

[6] S. Hattori and Y. Tanaka, Trans. JSME **68B**, 130 (2002).

[7] S. Hattori, Y. K. Goto and T. Fukuyama, Wear **260**, 1217 (2006).

[8] S. M. Ahmed, Wear **218**, 119 (1998).

[9] M. O. Barbaglia and F. J. Bonetto, J. Appl. Phys. **95**, 1756 (2004).

[10] M. Germano, A. Alippi, A. Bettucci, F. Brizi and D. Passeri, Ultrasonics **50**, 81 (2010).

[11] G. E. Vazquez and S. J. Putterman, Phys. Rev. Lett. **85**, 3037 (2000).

[12] A. Moshaii, S. Tajik-Nezhad and M. Faraji, Phys. Rev. E **84**, 046301 (2011).

[13] Y. Zhang, A. Sam and J. A. Finch, Coll. Surf. A: Physicochem. Eng. Aspects **223**, 45 (2003).

[14] T. Okawa, T.Tanaka, I. Kataoka and M. Mori, J. Heat Mass Tran. **46**, 903 (2003).

[15] J. Lu, R. Q. Xu, X. Chen, Z. H. Shen, X. W. Ni, S. Y. Zhang and C. M. Gao, J. Appl. Phys. **95**, 3890 (2004).

[16] Xiumei Liu, Youfu Hou, Xinhua Liu, Jie He, Jian Lu and Xiaowu Ni, Optik **122**, 1254 (2011).